Phytoplankton and Primary Production in the Red Sea

27

Mohammad Ali B. Qurban, Mohideen Wafar and Moritz Heinle

Abstract

Studies on phytoplankton and primary production in the Red Sea are few and far between, and even in the few that have been conducted, most cover only a limited area. The last review of phytoplankton and primary production by Ismael (2015) reaffirmed the oligotrophic nature of the Red Sea and the north-to-south increasing trend in chlorophyll concentrations and rates of primary production. Also, in the above review the inventory of phytoplankton species was enlarged to 389 from the earlier record of 181 by Halim (1969). Since then, four research cruises undertaken in the Saudi Arabian waters of the Red Sea (2012–2015) have added a considerable amount of data on the patterns of primary production in the Red Sea and this review builds on that of Ismael (2015) by presenting the new findings. The levels of biomass and production in the Red Sea are relatively low, with a discernable north-south gradient. Their distribution is influenced by anticyclonic eddies, which entrain the nutrient-rich Gulf of Aden Intermediate Water across the Red Sea basin. Biomass and production in regions of eddy currents are twice as high as those elsewhere, suggesting that the notion that the Red Sea is oligotrophic needs to be revised. The injection of nutrients into the euphotic zone in the eddy boundary currents favours the proliferation of producers across a range of size classes rather than of a single class. As with any nutrient-poor tropical sea, the primary production in the Red Sea is supported up to 80% by nano- and picoplankton. Though the contributions of microplankton (diatoms and dinoflagellates) appear to be less significant, the phytoplankton diversity is quite high. With additional records of 74 species from the samples in the four cruises, the current inventory of phytoplankton stands at 463 species. The review also provides suggestions on prospective avenues of phytoplankton research in the Red Sea waters. These include extensive spatial and seasonal coverage of primary production, the importance of benthic production, a better evaluation of nitrogen (N) fixation by *Trichodesmium* spp., the role of allochthonous nutrient sources (such as dust) in increasing the productivity, additional inventories of phytoplankton species, especially those belonging to the nano- and picoplankton size classes, and the assessment of the importance of the heterotrophy and microbial loop in the food chain dynamics. Experimental studies on the physiology of phytoplankton that already live at extreme conditions of temperature and salinity in the Red Sea could also help to understand how phytoplankton in other seas would react to the effects of global warming and climate change.

Introduction

The Red Sea is a narrow (maximum width of 355 km) marginal sea of the northwest Indian Ocean, located between 12.5°N and 30°N, occupying an area of 4.51×10^5 km^{2}with a seawater volume of ~233,000 km^3 (average depth 490 m). In the north, the main body of the Red Sea branches off to the Gulf of Suez to the northwest and the Gulf of Aqaba to the northeast. In the south, the Red Sea is connected to the Arabian Sea through the Strait of Bab al Mandeb. The sill depth of ~125 m of the Strait of Bab al Mandeb restricts the main body of water of the Red Sea from exchanging freely with the waters of the Gulf of Aden.

The oceanographic setting and the extreme paucity of oceanographic data should be taken into consideration when the literature on phytoplankton and primary production of

M. A. B. Qurban (✉) · M. Wafar · M. Heinle
Center for Environment & Water, Research Institute, King Fahd University of Petroleum and Minerals, Dhahran, Saudi Arabia
e-mail: mqurban@kfupm.edu.sa

M. A. B. Qurban
Geosciences Department, King Fahd University of Petroleum and Minerals, Dhahran, Saudi Arabia

N. M. A. Rasul and I. C. F. Stewart (eds.), *Oceanographic and Biological Aspects of the Red Sea*,
Springer Oceanography, https://doi.org/10.1007/978-3-319-99417-8_27

the Red Sea waters is reviewed. The Red Sea is one of the warmest and saltiest water bodies, mainly due to the absence of freshwater inflow to any part of the basin, and high evaporation rates, especially in the northern part, which could be as high as 210 cm $year^{-1}$ (Edwards 1987). Meridional circulation of the Red Sea involves the convective sinking of dense waters in the northern basin, their flow southward along the bottom of the basin, and their escape into the Gulf of Aden at the Strait of Bab al Mandeb. The compensatory flow of the meridional circulation is from the Gulf of Aden into the Red Sea, which includes the movement of surface waters for part of the year (winter-spring) and subsurface Gulf of Aden Intermediate Water (GAIW) for the rest (summer-autumn). The GAIW is rich in nutrients and thus is the only source of nutrients needed to sustain the phytoplankton productivity of the otherwise oligotrophic Red Sea waters (Souvermezoglout et al. 1989; Churchill et al. 2014; Wafar et al. 2016a). Oceanographic data on the Red Sea waters are scarce. Even though the marine resources of the Red Sea are shared by eight countries (Saudi Arabia, Egypt, Sudan, Eritrea, Yemen, Israel, Jordan and Djibouti, in that order of area of territorial waters), only a few oceanographic surveys have been conducted. The extent of the paucity of data is signaled by the following comparisons. The oceanographic database for the Indian Ocean at the National Institute of Oceanography, India, indicates the following: (i) hydrography data are available only for seventy stations in the Red Sea as against the 13779 stations in the rest of the Indian Ocean, and (ii) data on chemical and biological parameters are not available from the Red Sea as against those primary production parameters from 2790 stations and on nutrients from 4878 stations in the rest of the Indian Ocean. While the numbers themselves may not be precise, they are still indicative of the severity of the paucity of data.

A single primary production dataset can provide information on how productive an ecosystem is. However, the study of primary production during a multidisciplinary oceanographic cruise also reveals information on what physical and chemical parameters control primary production and how. Until 2012, when the King Fahd University of Petroleum and Minerals, Saudi Arabia, undertook several multidisciplinary cruises for four years in the Saudi Arabian waters of the Red Sea, almost all the data available on primary production in the main body of the Red Sea were from scattered measurements. Hence the data from measurements in the main body of the Red Sea prior to 2012 and after 2012 are reviewed separately in the following sections. The data for the Gulf of Suez and the Gulf of Aqaba are also discussed separately.

Overview of the Results

Main Body of the Red Sea

Before 2012

The earliest estimates of primary production (arrived at from chlorophyll and surface-incident solar radiation data) were made by Yentsch and Wood (1961) at five stations during the *Atlantis* cruise in 1958. The levels of biomass (0.1–0.7 µg Chl *a* L^{-1}) and production (11–34 mg C m^{-2} h^{-1}) determined by them were low. However, interestingly, the data also showed that the biomass and production at the station in the southern Red Sea (15.5ºN) were twice as high (up to 0.7 µg Chl *a* L^{-1} and 34 mg C m^{-2} h^{-1}) as those at the other four stations (less than 0.35 µg Chl *a* L^{-1} and 20 mg C m^{-2} h^{-1}) to the north (17.5 to 27.6ºN). The vertical distribution of chlorophyll also showed deep chlorophyll maxima (DCM) at about 80 m at the five stations.

Similar properties of low levels of production and a north-south gradient were also evident in the data gathered subsequently by Khmeleva (1970) and Petzold (1986). The data presented by Khmeleva (1970) showed that the primary production rate ranging from 17.5 mg C m^{-2} h^{-1} in the northern Red Sea to 33 mg C m^{-2} h^{-1} in the central Red Sea dramatically increased to 133 mg C m^{-2} h^{-1} in the southern Red Sea. Measurements made by Petzold (1986) showed still lower levels of production, ranging from 6 to 63 mg C m^{-2} h^{-1}. Remarkably, these data also demonstrated a north-south gradient, with a rate of primary production less than 11 mg C m^{-2} h^{-1} in the central and northern Red Sea, increasing to 63 mg C m^{-2} h^{-1} in the southern Red Sea. Similarly, average column-integrated phytoplankton biomass values obtained by Petzold (1986) also increased from north to south, from 24.3 through 38.8 to 59.2 mg Chl *a* m^{-2}. Weikert (1987) reaffirmed these characteristics in his review of plankton of the Red Sea and tentatively concluded that the inflow of nutrient-rich surface and sub-surface GAIW from the Gulf of Aden into the Red Sea is responsible for the establishment of this gradient. He also acknowledged the paucity of data: "The continued shortage of quantitative data is most obvious in the field of primary production. The traditional concept that most of the Red Sea is oligotrophic or even ultra-oligotrophic has not yet been verified in a true scientific sense". It is only three decades later that the traditional concept of the Red Sea has been changed (see below).

Other studies in the main body of the Red Sea have reported higher concentrations of biomass and rates of production. These include those of Shaikh et al. (1986) at two stations close to Jeddah, Khomayis (2002) in the coastal waters off Jeddah, and Al-Harbi and Khomayis (2010) in severely polluted waters near Jeddah. The averages of production rates measured by Shaikh et al. (1986) were 82.5 mg C m^{-2} h^{-1} at the inshore station and 96.3 mg C m^{-2} h^{-1} at the offshore station, with biannual peaks at both sites. In the other two studies conducted at sites close to the Saudi Arabian coast, only Chl *a* was measured. Khomayis (2002) reported concentrations ranging from 0.31 to 2.08 μg Chl *a* L^{-1} and Al-Harbi and Khomayis (2010) reported much higher values for severely polluted waters. Proximity to the coast and possible runoff of nutrients from urban sources are most likely responsible for sustaining higher production rates in the waters near Jeddah. On the other hand, measurements made by Fahmy (2003) at 15 stations in the Egyptian coastal waters showed that the concentrations of Chl *a* ranged only between 0.09 and 0.18 μg L^{-1}, with an annual average of 0.13 μg L^{-1}.

Besides the above, several studies (Yentsch 1965; Lenz et al. 1988; Baars et al. 1998) have also reported on chlorophyll and primary production from the extreme southern part of the Red Sea, obtained as part of data acquisition in the northwest Indian Ocean, rather than as targeted studies on the Red Sea.

Apart from in situ measurements, remote sensing at a basin-scale was also used to determine the levels of chlorophyll concentrations and their variations (Longhurst et al. 1995; Acker et al. 2008; Elawad 2012; Raitsos et al. 2013). These were useful in demonstrating basin-scale spatial and temporal variations of chlorophyll and Chl-derived primary production.

After 2012

Between 2012 and 2015, scientists from the King Fahd University of Petroleum and Minerals, Saudi Arabia, undertook four cruises in the Saudi Arabian waters of the Red Sea (Fig. 27.1) during different seasons and simultaneously collected data on physical, chemical, and biological properties. In addition, they also measured primary production using stable and radioactive isotopes. The dataset thus generated is the largest ever from the Red Sea on biomass and production of phytoplankton and has been useful in advancing our knowledge of phytoplankton production processes in the Red Sea (Qurban et al. 2014, 2017; Wafar et al. 2016a, b; Wafar 2016). In the following sections, these data are summarized, highlighting the significant findings.

Physical Settings

Maillard and Soliman (1986) found that eddy circulations are superimposed on the meridional circulation in the Red Sea. Since then, two studies (Quadfasel and Baunder 1993; Zhan et al. 2014) have shown that eddies occur over the entire Red Sea basin, with most of them anticyclonic and some of them quasi-permanently present. The 1100 km long hydrographic section presented by Wafar et al. (2016b) showed a series of three depressions of isotherms from 17ºN to 27ºN along the axis of the Red Sea basin (Fig. 27.2a). Data on directions and velocity of the currents acquired at the same time showed three pairs of alternating zonal currents (Fig. 27.2b), each bracketing the depressions of isotherms. Taken together, these provide evidence for three successive anticyclonic eddies between 17ºN and 27ºN (Wafar et al. 2016b).

Nutrients

Remarkably, the distribution of nutrients in the same section followed a pattern of alternating high and low concentrations (Fig. 27.3) and the locations of high concentrations matched closely those of the zonal currents shown in Fig. 27.2 (Wafar et al. 2016a). The high column concentration of nutrients in the region of the zonal currents also results in advective/diffusive fluxes of nutrients into the euphotic zone. The extent of these fluxes is such that the concentrations are higher by up to an order of magnitude or more at the boundaries of the eddies than at their centre. The patterns of the distribution of nutrients are thus governed predominantly by eddy, rather than meridional, circulations (Wafar et al. 2016b).

Chlorophyll a

Except for a coastal station along 17ºN, the concentrations of Chl *a* measured in the four cruises were less than 1 μg L^{-1} (Fig. 27.4). While a north-south gradient can be perceived even within these low concentrations, plotting the measurements from the euphotic zone depths as surface values against the latitudes showed alternating bands of high and low Chl *a* concentrations (Fig. 27.5). The high values are at the locations of the zonal currents, with a continuity of higher concentrations along the eastern coast between the two zonal currents. What is even more interesting is the near-perfect alignment of the high concentrations of column-integrated Chl *a* with the locations of zonal currents, separated by lower values of concentration (Fig. 27.6).

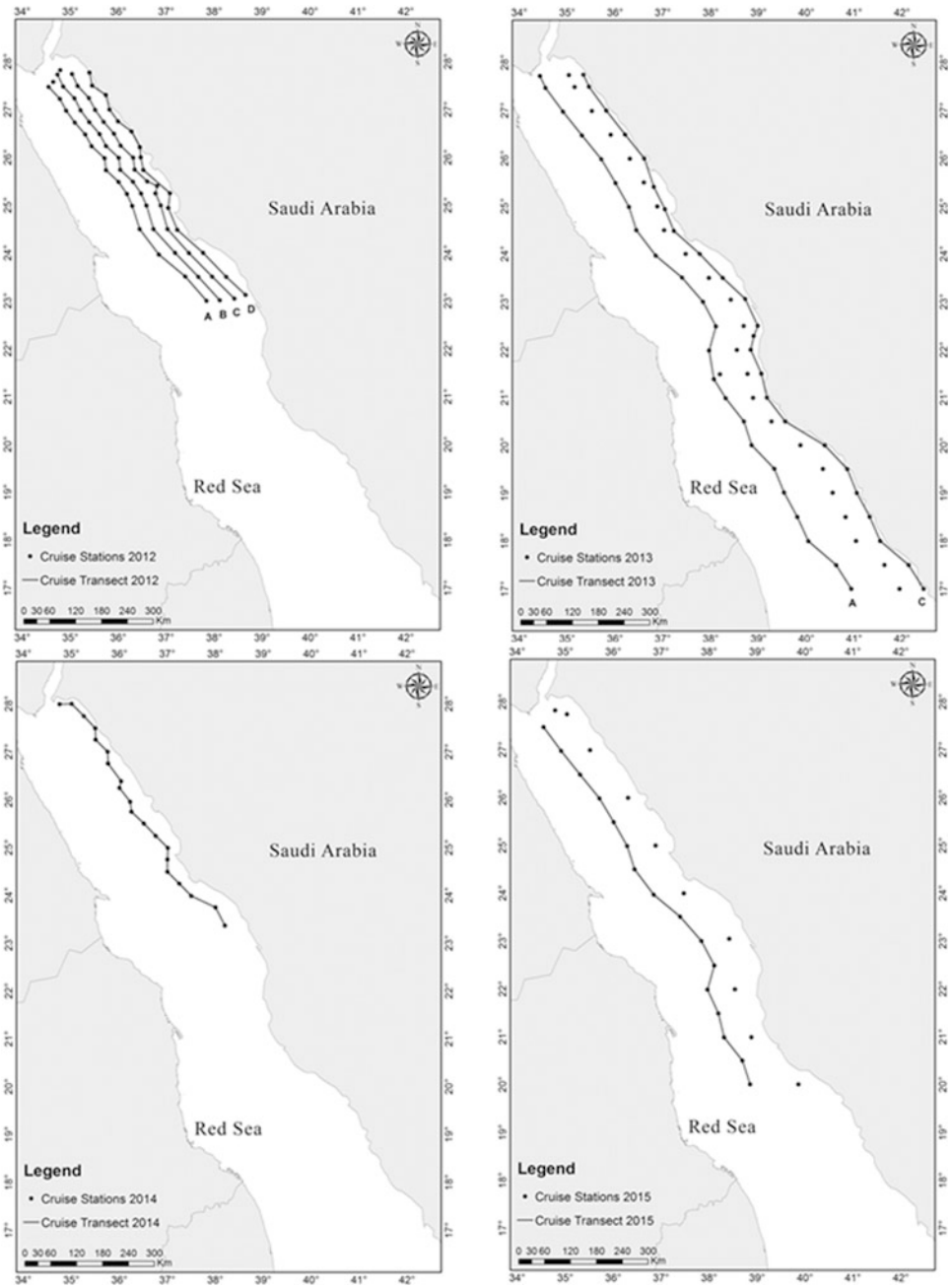

Fig. 27.1 Locations of the stations occupied and the layout of the transects during the four cruises from 2012 (top left) to 2015 (bottom right)

Carbon Uptake

Carbon uptake from all depths in the 2012 and 2013 cruises showed that the phytoplankton production is quite low. Carbon uptake was less than 1 μg C L^{-1} h^{-1} down to 24ºN and then increased to 1–4 μg C L^{-1} h^{-1} until 17ºN (Fig. 27.7). The uptake rates were significantly higher between 23ºN and 23.5ºN. As was observed with Chl *a*, there were alignments of high column-integrated carbon uptake rates with the locations of zonal currents, separated by lower values (Fig. 27.8).

Cell Counts

Qurban et al. (2017) also enumerated microplankton cell counts using optical microscopy, and nanoplankton and cyanobacterial cell counts using flow cytometry. Plots of these as a function of the direction of the zonal currents (Fig. 27.9) also showed high densities at the location of the currents separated by lower densities.

The patterns of distribution of chlorophyll, phytoplankton cell densities and primary production matching with those of nutrients and zonal currents, thus led Qurban et al. (2017) to

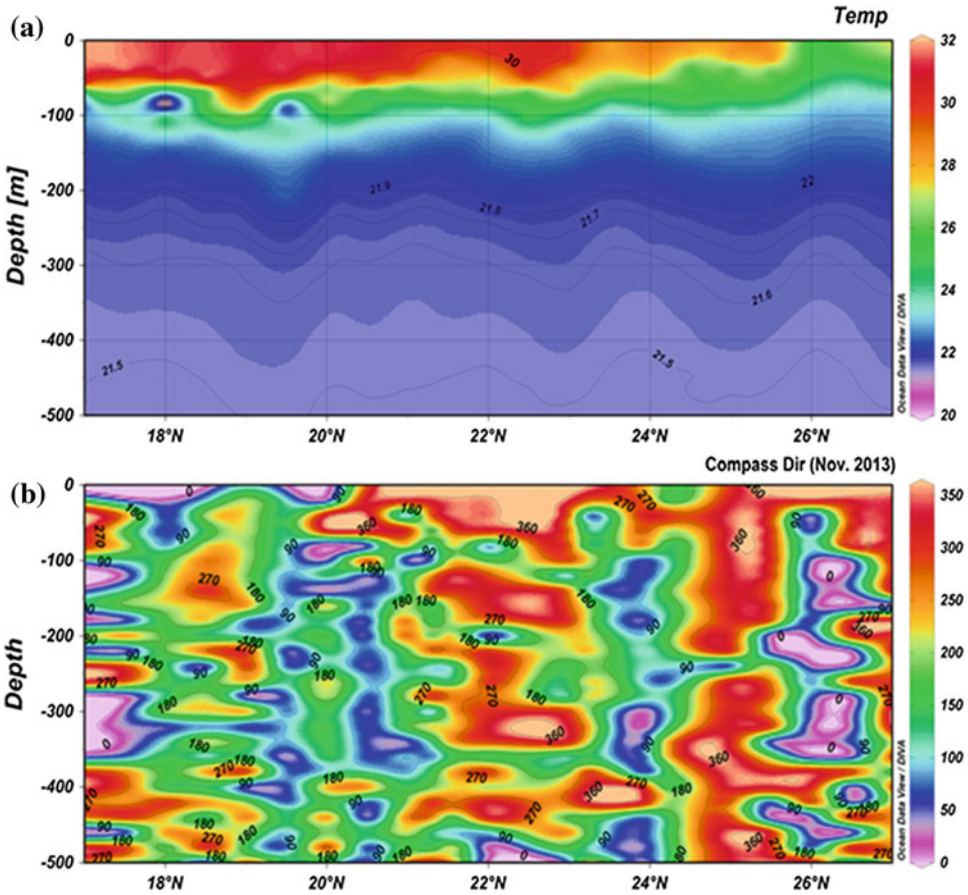

Fig. 27.2 Distribution of **a** potential temperature and **b** directions of zonal currents between 0 and 500 m between 17ºN and 27ºN along the axis of the Red Sea in November 2013

conclude that the anticyclonic eddy circulations have a determining effect on phytoplankton biomass and production in Red Sea.

Depth of Chlorophyll Maximum (DCM)

Deep chlorophyll maxima were apparent in all five chlorophyll profiles published by Yentsch and Wood (1961). Interestingly, the depth at which the DCM was detected in the four central and northern stations was about 80 m, whereas it was 60 m in the single station in the south. Strong deep chlorophyll maxima were present in chlorophyll profiles at all stations sampled by Qurban and his colleagues (n = 159) with a north-south gradient, with the DCM occurring at deeper locations (>70 m) north of 22–24ºN than in the south (<70 m) (Fig. 27.10). The concentration of Chl *a* at the DCM was, in most of the stations, significantly higher than that in the euphotic zone. Also, the rates of carbon uptake measured at the DCM consistently exceeded those measured at 1% light intensity at all stations (Fig. 27.11), indicating that the sites of the DCM have a significant contribution to the primary production in the Red Sea.

Phytoplankton Size Fractions

While reviewing published results on phytoplankton in the Red Sea, Weikert (1987) noted that the largest proportion of phytoplankton was composed of very small planktonic cells less than 60 µm in diameter and that larger microplankton species were rare. While the results shown in Fig. 27.9 agree with the above findings, fractionation of smaller cells in flow cytometry shows that cyanobacteria (Prochlorococcus sp. and Synechococcus sp.) and picoeukaryotes are far more abundant than nanoplankton cells (Fig. 27.12). Interestingly, in their vertical distribution from the surface down to the depth of the DCM in the stations along the axis, a niche separation exists. The cyanobacterial cells are dominant in the top layers down to about 20 to 30 m whereas the nanoplankton and picoeukaryotes are dominant at depths greater than 30 m and down to the depth of the DCM. Even though the smaller cells are better adapted to low-nutrient conditions, the niche separation between the pro- and eukaryotes in this section is remarkable.

The preponderance of smaller cells also translates into proportionally higher biomass and productivity in the smaller cell fraction. Carbon uptake measured at 9 stations in the 2012 cruise showed that the contribution by the <20 µm

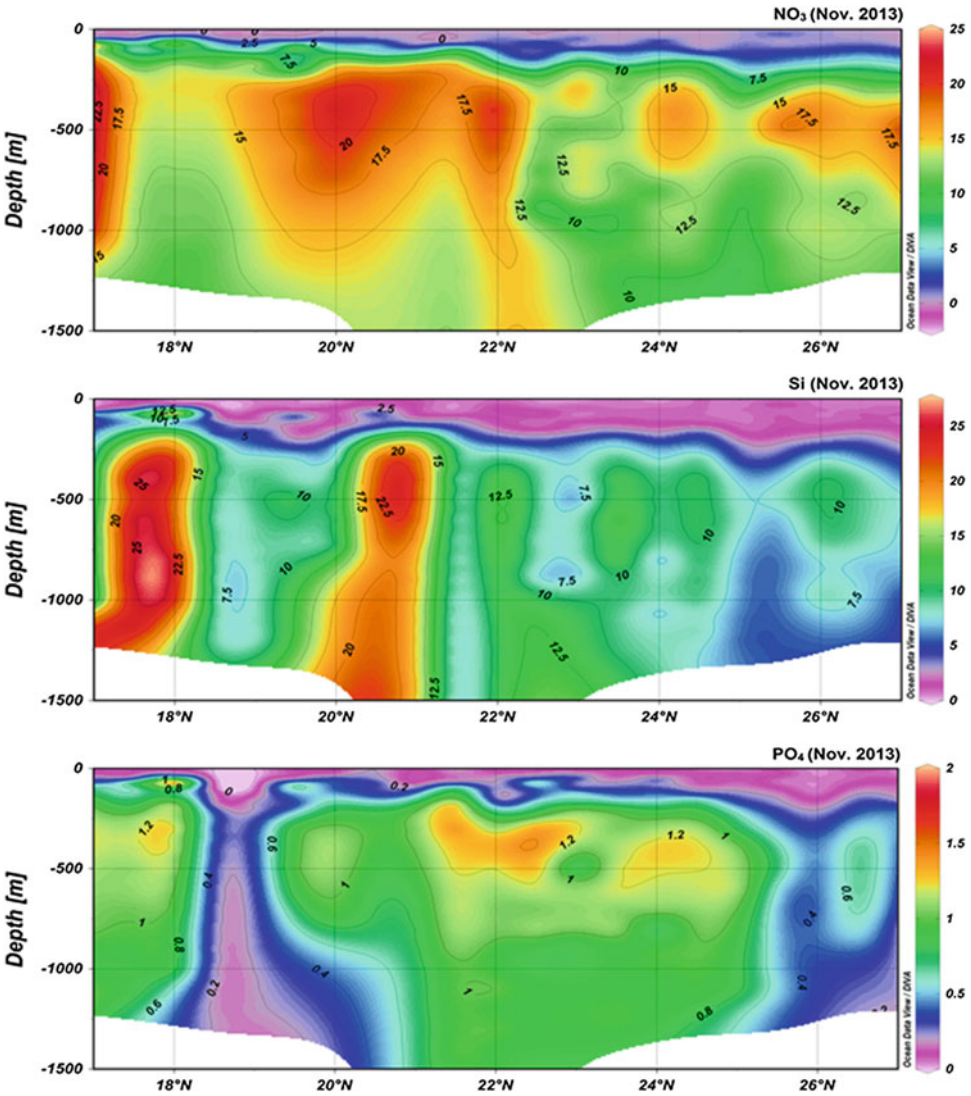

Fig. 27.3 Distribution of **a** NO_3-N, **b** $Si(OH)_4$-Si and **c** PO_4-P between 0 and 1500 m between 17ºN and 27ºN along the axis of the Red Sea in November 2013

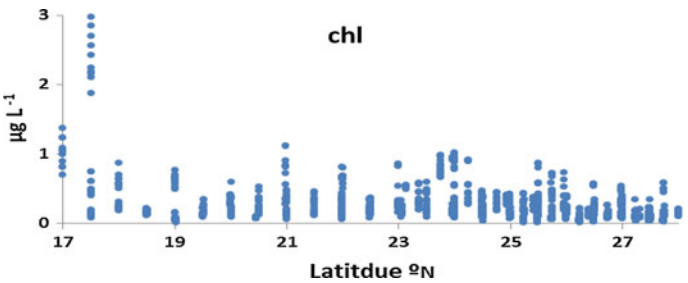

Fig. 27.4 Spatial variability in chlorophyll *a* (chl *a*) concentrations during the 4 cruises (2012–2015)

fraction to the uptake in unfractionated samples ranged from 68 to 91% (average ± SD of 81 ± 0.09%) (Fig. 27.13a). When the <20 µm fraction was further fractionated to nano- (2–20 µm) and picoplankton (<2 µm) in the 2013 cruise, it emerged that the carbon uptake by picoplankton almost consistently exceeded that of nanoplankton. Carbon uptake by picoplankton accounted for 60 ± 12% of the uptake in the <20 µm fraction (Fig. 27.13b). The data from the 2015 cruise also showed that the biomass and carbon uptake rates in the picoplankton fraction consistently exceeded those in the nanoplankton fraction, accounting for between 70 and 90% of the values measured in the <20 µm fraction (Fig. 27.13c, d).

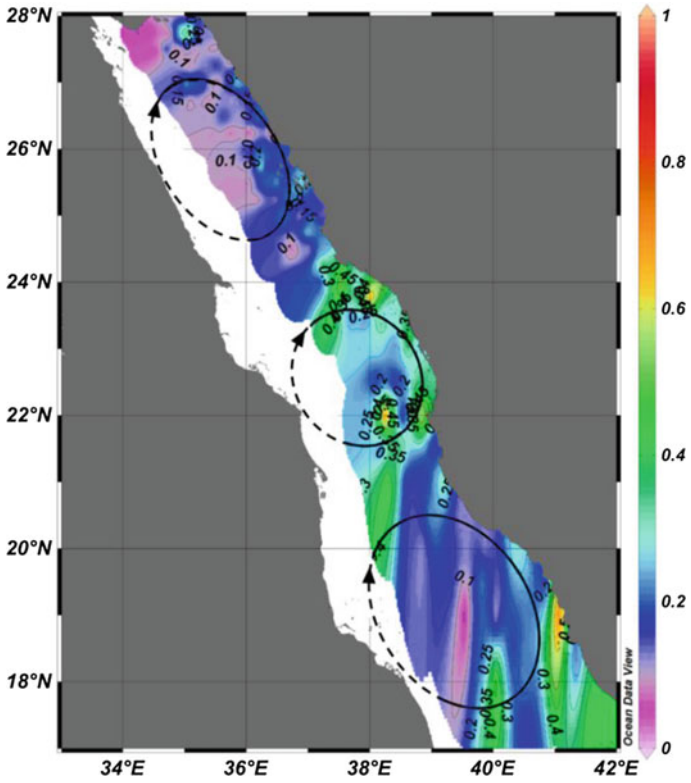

Fig. 27.5 Spatial distribution of the concentrations of Chl *a* (ug L^{-1}) from the euphotic zone depths for all 4 cruises combined

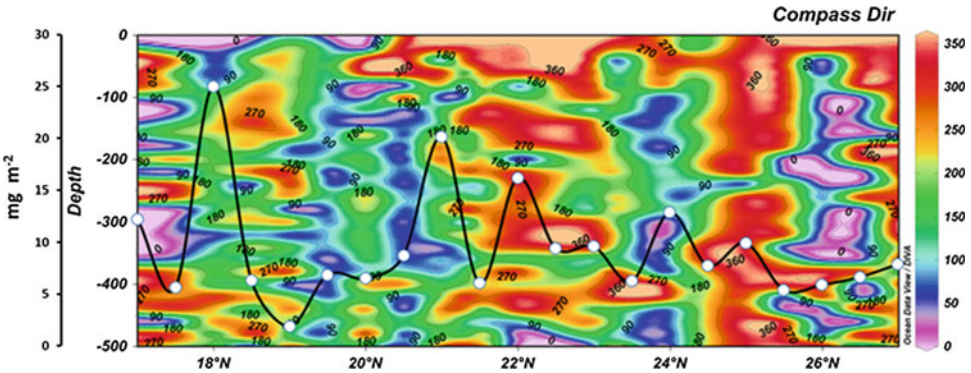

Fig. 27.6 Chl *a* distributionsuperimposed on the plots of the compass directions of the flows in the depth range of 0–500 m between 17 and 27ºN along the axis of the Red Sea basin during the 2013 cruise

Nitrogen Uptake

Ever since the finding that diatoms prefer nitrate-rich environments (Malone 1980), there have been many reports of new N (nitrate) uptake by large cells and regenerated N (ammonium and urea) uptake by smaller cells (Dham et al. 2005). Consistent with the dominance of smaller cells in phytoplankton, uptake of regenerated N accounted for about 80% of the total N uptake measured in the 2012 and 2013 cruises (Fig. 27.14). In both cruises, the uptake rates of all three N compounds significantly correlated with their concentrations rather than with Chl *a*, demonstrating that N uptake, and hence the primary production, is controlled by nutrient availability.

^{13}C Uptake

^{13}C can also be used to measure carbon uptake by phytoplankton. Using ^{13}C instead of ^{14}C has the advantage that ^{13}C can be used together with ^{15}N in the same incubation providing more reliable data for the C:N uptake ratio than when ^{14}C and ^{15}N are used independently. Qurban and his colleagues investigated the applicability of using ^{13}C and ^{14}C to determine the primary production in the Red Sea waters. A Model II regression relating the uptake rates measured with both these isotopes (Fig. 27.15) showed that $\rho^{14}C = 0.97\ \rho^{13}C + 0.09$ ($r = 0.89$; n = 11). The closeness of the slope to unity, as was found in a similar study by

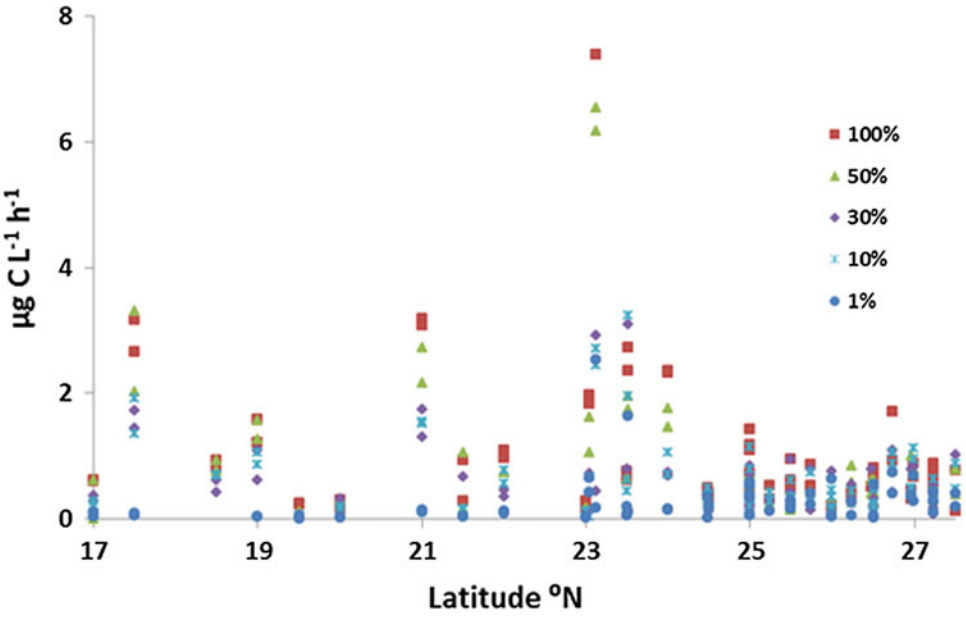

Fig. 27.7 Spatial distribution of the carbon uptake rates at different light depths (100%, 50%, 30%, 10% and 1%) in the 2012 and 2013 cruises

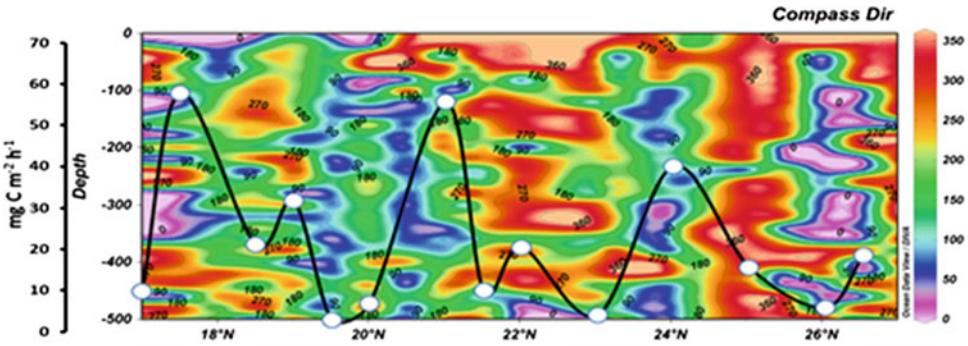

Fig. 27.8 Distribution of column-integrated rates of primary production superimposed on the plots of the direction of the currents between 17 and 27ºN along the axis of the Red Sea basin during the 2013 cruise

Slawyk et al. (1977), indicates that ^{13}C can be used simultaneously with ^{15}N to determine the C and N turnover rates in these waters, and is a useful alternative when radioactive tracers cannot be procured.

Phytoplankton

Species Composition

Ismael (2015) reviewed the reports on the composition of the phytoplankton species and related studies in the Red Sea and catalogued 389 species and varieties, with the diversity of dinoflagellates (168 species) greater than that of diatoms (137 species). An additional 29 genera were recorded from the samples collected during the four KFUPM cruises in the Red Sea between 2012 and 2015 (Table 27.1). Combining the list of genera compiled by Ismael (2015) and those recorded since then (Table 27.1), the current inventory of phytoplankton genera in the Red Sea stands as follows: (i) 62 genera of bacillariophytes (diatoms), (ii) 44 genera of dinophytes (dinoflagellates), (iii) 10 genera of cyanophytes (blue-green algae), (iv) 2 genera of dictyophytes (silicoflagellates), (v) 2 genera of chlorophytes (green algae), and (vi) one genus of cryptophytes.

Part of the samples collected in the 2012 cruise was also subjected to species level identification. This added new records of 74 species (Table 27.2) to those already compiled by Ismael (2015). Taken together, the current inventory of phytoplankton species of the Red sea and the Gulfs of Aqaba and Suez now stands at 463 species.

Spatial Variations

Almost all of the studies reviewed by Ismael (2015) are those where samples were obtained only from a few stations. Thus, other than the seasonal study conducted by Shaikh et al. (1986), little is known about the distribution patterns, both on spatial and temporal scales. The data from the 2012

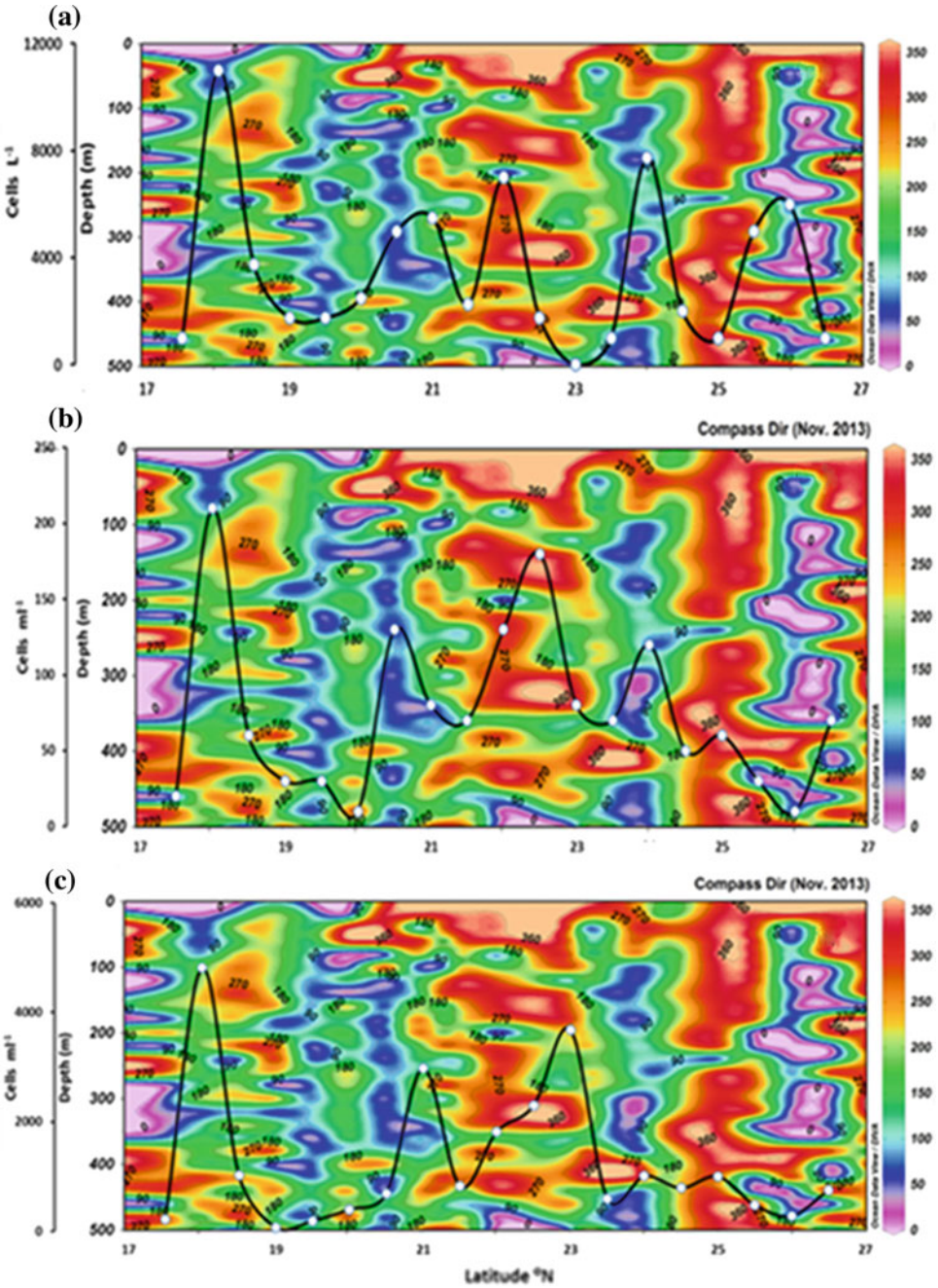

Fig. 27.9 Latitudinal changes in the densities of **a** microplankton (cells L^{-1}), **b** nanoplankton (cells mL^{-1}), and **c** cyanobacteria (cells mL^{-1}) at a depth of 10 m superimposed on the plots of the direction of the currents along the axis of the Red Sea basin during the 2013 cruise

cruise of KFUPM showed a higher numerical abundance of diatoms and dinoflagellates in the offshore transect along the axis of the basin between 23ºN and 27ºN, as compared to that in a nearshore transect a few km from the coast (Fig. 27.16). The latitudinal variations within the Red Sea associated with eddy circulations deduced in the 2013 cruise are also evident in the data from the 2012 and 2015 cruises (Fig. 27.17). The localized proliferation of phytoplankton in the Red Sea is due to the injection of nutrients from the shallow Gulf of Aden into the euphotic zone, transported in anticyclonic eddy circulations across the Red sea basin (Qurban et al. 2017).

Temporal Variations

The data of Shaikh et al. (1986) from the offshore station near Jeddah clearly showed two peaks of phytoplankton abundance—one in winter and one in summer. A plot of the data collected during three different seasons (November

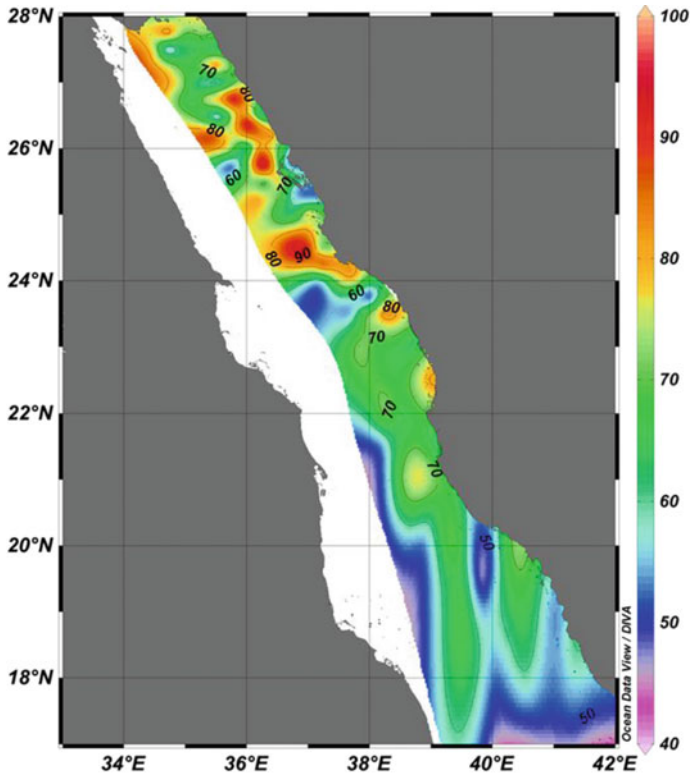

Fig. 27.10 Distribution of the depth of DCM between 17º and 27ºN

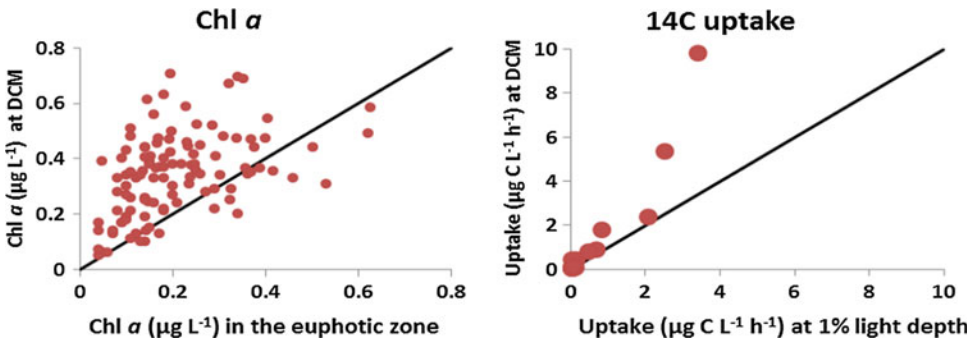

Fig. 27.11 Plots of the concentration of Chl *a* at the DCM against the column-integrated Chl *a* concentration within the euphotic zone and of the carbon uptake rate at the DCM against the uptake rate at 1% light depth at all stations. 1:1 lines are also shown for comparison

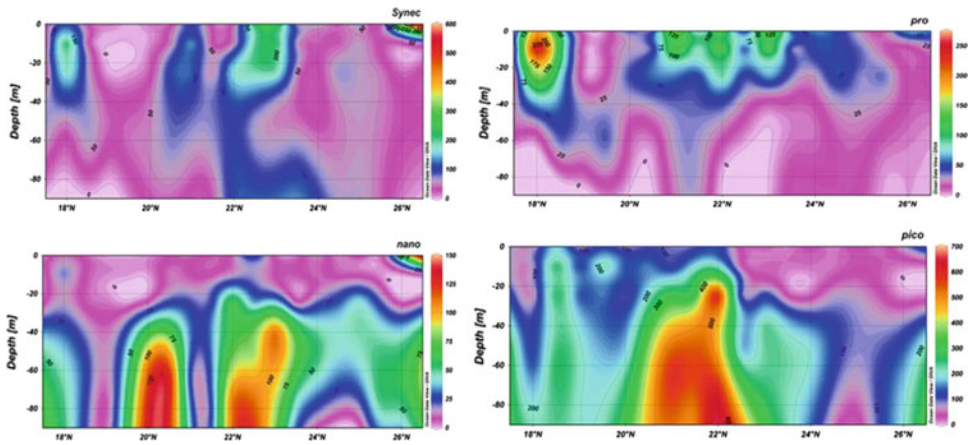

Fig. 27.12 Vertical distribution of the density of Synechococcus, Prochlorococcus, nanoplankton and picoeukaryotes between 17ºN and 27ºN along the axis of the Red Sea basin in the 2013 cruise

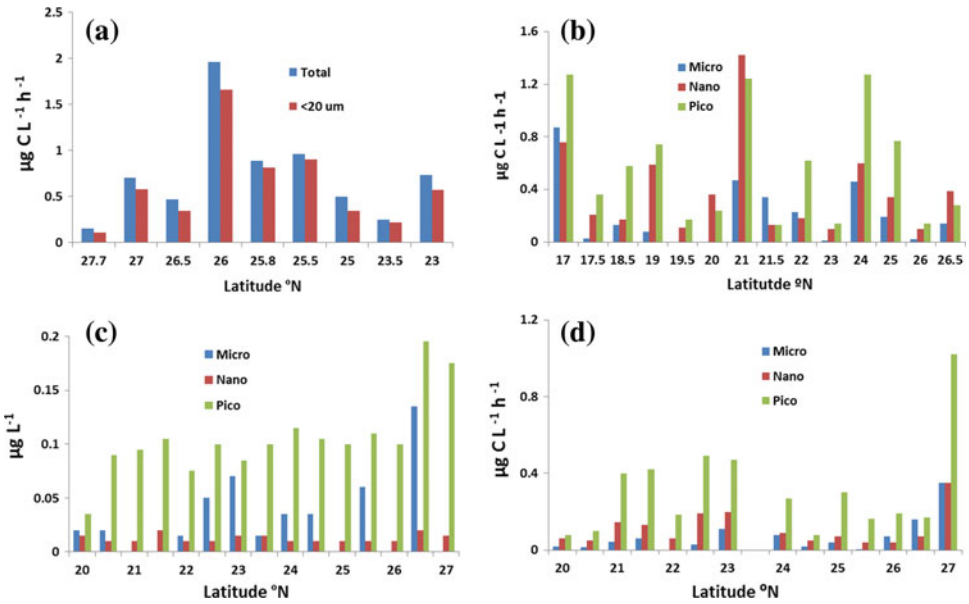

Fig. 27.13 Size fractionated biomass and carbon uptake in the Red Sea. **a** 2012 cruise, **b** 2013 cruise and, **c** and **d** 2015 cruise

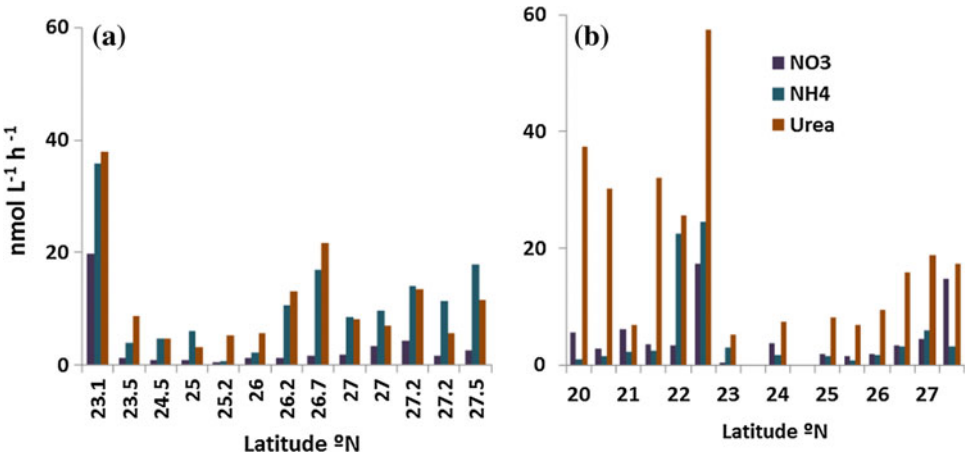

Fig. 27.14 Rates of uptake of nitrate, ammonium, and urea measured during the cruises in **a** 2012 and **b** 2013

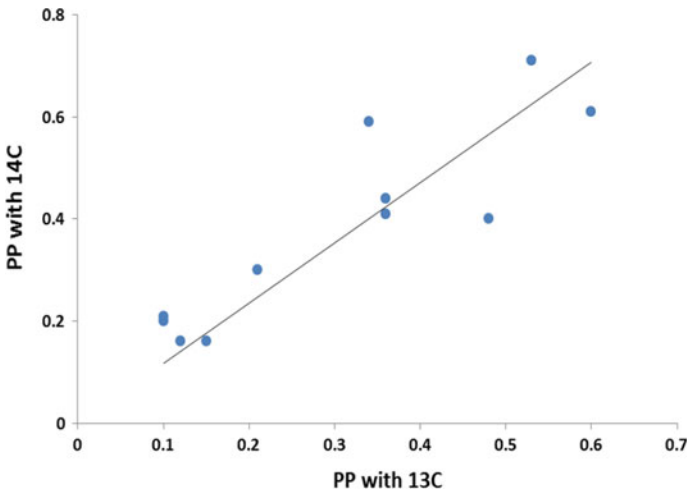

Fig. 27.15 Relationship between the carbon uptake rates determined with ^{14}C and ^{13}C

Table 27.1 Genera of phytoplankton recorded in the Red Sea since the compilation by Ismael (2015)

Bacillariophytes	16. *Cochlodinium*
1. *Bellerochea*	17. *Corythodinium*
2. *Ditylum*	18. *Karenia*
3. *Entomoneis*	19. *Katodinium*
4. *Fragilaria*	20. *Lingulodinium*
5. *Gossleriella*	21. *Peridinium*
6. *Gomphonema*	22. *Scrippsiella*
7. *Haslea*	23. *Tripos*
8. *Licmophora*	24. *Torodinium*
9. *Lithosdesmium*	**Cyanophytes**
10. *Plagiotropis*	25. *Anabaena*
11. *Pseudosolenia*	26. *Nostoc*
12. *Synedropsis*	27. *Spirulina*
13. *Trachyneis*	28. *Snowella*
Dinophytes	**Chlorophytes**
14. *Achradina*	29. *Pterosperma*
15. *Alexandrium*	

2013, June 2014, and March 2015) between 23ºN and 27ºN showed near-similar values in autumn-winter and distinctly higher values in the summer (Fig. 27.18). Thus, notwithstanding the tropical nature and the low production capacity, the abundance of phytoplankton over a larger area of the Red Sea could vary seasonally.

Gulf of Aqaba

The narrow (maximum width of 24 km) Gulf of Aqaba is a 160 km northeast extension of the Red Sea separated from the latter by the Strait of Tiran with a sill depth of ~240 m at 28ºN. The Gulf is bordered by Saudi Arabia to the east and Egypt to the west, except at the northern extremity where it is bordered by Jordan and Israel. Current knowledge about the phytoplankton biomass and primary production in the Gulf of Aqaba is attributable to studies conducted mainly in the Jordanian waters and from a series of stations occupied in a transect in the Gulf of Aqaba by an Israeli research team. Besides these, some measurements have also been made at isolated locations.

The studies in the Jordanian waters have been mainly conducted by Badran and his team. Badran and Foster (1998) determined Chl *a* over an annual cycle at four stations in the inshore waters and found that the concentrations at 3 of them were well below 1 μg L^{-1}, with seasonally higher values in the winter than in the summer. The concentrations and seasonal pattern differed only at a station located within the port. The maximum concentration was up to 4.5 μg L^{-1} and it was associated with an early spring-summer bloom. In a subsequent study at an offshore station, Badran (2001) found that the Chl *a* concentrations in the water column rarely exceeded 0.4 μg L^{-1} except for an instance in late winter when the concentration increased to 1.2 μg L^{-1}. The vertical distribution was more or less uniform in the autumn to spring period but was characterized by a strong subsurface maximum in summer. Rasheed et al. (2002) measured Chl *a* concentrations again at the same station as sampled by Badran in 2001 and at several inshore stations over a reef. They found that, while the concentrations generally remained less than 0.4 μg L^{-1} offshore, there was a notable increase over the reef stations. In a later study, Badran et al. (2005) analyzed Chl *a* records from 1994 to 2000 and found that summer concentrations were generally less than 0.4 μg L^{-1} and winter concentrations higher. Summing up, the phytoplankton biomass is very low in Aqaba waters except when affected by anthropogenic addition of nutrients and that the seasonal cycle is characterized by blooms in winter, rather than in summer.

Three major publications from the Israeli team are those of Levanon-Spanier et al. (1979), Labiosa et al. (2003), and Stambler (2005). Levanon-Spanier measured Chl *a* and the primary production at three stations in the axis of the Gulf. They found that the biomass varied from 0.02 to 0.45 μg L^{-1}, with values higher in winter than in summer, and that the rates of primary production ranged between 0.05 and 3.38 μg C L^{-1} h^{-1}, with a seasonality similar to that observed for biomass. In a study combining field data and remotely-sensed data, Labiosa et al. (2003) found that phytoplankton communities in the Gulf are characterized by a large bloom in spring and a small bloom in autumn, with the

Table 27.2 List of phytoplankton species recorded in the northern Red Sea since the compilation by Ismael (2015)

Bacillariophyta	**Dinoflagellates**
1. *Actinoptychus undulatus*	34. *Alexandrium catenella*
2. *Asteromphalus hookeri*	35. *Alexandrium minutum*
3. *Bacteriastrum delicatulum*	36. *Alexandrium ostenfeldii*
4. *Chaetoceros denicus*	37. *Ceratium belone*
5. *Chaetoceros densus*	38. *Ceratium biceps*
6. *Chaetoceros lauderi*	39. *Ceratium candelabrum*
7. *Chaetoceros tenussimus*	40. *Ceratium carriense*
8. *Chaetoceros teres*	41. *Ceratium furca*
9. *Cylindrotheca minimus*	42. *Ceratium fusus*
10. *Dactylosolen fragilisima*	43. *Ceratium gibberum*
11. *Ditylum brightwelli*	44. *Ceratium incisum*
12. *Entomoneis sulcata*	56. *Dinophysis infundibula*
13. *Eucamphia zodiacus*	57. *Dinophysis rapa*
14. *Gossleriella tropica*	58. *Dinophysis rotundata*
15. *Gramatophora marina*	59. *Dinophysis urceola*
16. *Haslea balaerica*	60. *Gyrodinium glyptobynchus*
17. *Hemiaulus hauckii*	61. *Gyrodinium spirale*
18. *Hemiaulus membranaceus*	62. *Histioneis costata*
19. *Leptocylindrus minimus*	63. *Histioneis hyalina*
20. *Mastogloia erythraea*	64. *Oxytoxum reticulatum*
21. *Navicula transistans*	65. *Oxytoxum subulatum*
22. *Navicula delicatula*	66. *Oxytoxum tesselatum*
23. *Nitzschia lorenziana*	67. *Podolampas elegans*
24. *Plagiotropis lepidoptera*	68. *Protoperidinium subcurvipes*
25. *Pleurosigma elongatum*	69. *Protoperidinium pyriforme*
26. *Pseudonitzschia longissima*	70. *Pyrocystis gerbautii*
27. *Richelia intracellularis*	**Dictyophyceae**
28. *Synedropsis hyperborea*	*71. Dictyocha elegans*
29. *Thalasiossira hendeyi*	72. *Dictyocha speculum*
30. *Thalasiossira rotata*	*73. Octactis octonaria*
31. *Thalassionema frauenfeldii*	**Chlorophyta**
32. *Thalassionema nitzschoides*	74. *Pterosperma moebii*
33. *Thalassiosira nordenskioeldii*	

average concentrations during the bloom being twice as high as the pre-bloom conditions (0.3 to 0.5 μg L^{-1}). In a study of bio-optics along the axis of the Gulf, Stambler (2005) found that the concentrations of Chl *a* remained consistently less than 0.4 μg L^{-1}.

Dorgham et al. (2012) determined the concentrations of Chl *a* down to 100 m at a coastal station (Sharm El-Sheikh) at the Strait of Tiran over an annual cycle and observed that the concentrations ranged from 0.1 to 0.33 μg L^{-1}. The only instance when they were high (up to 1.2 μg L^{-1}) was in the spring at depths >70 m.

All the above studies demonstrate that the Gulf of Aqaba waters are oligotrophic, with the highest concentrations of Chl *a* rarely exceeding 0.4 μg L^{-1}.

Gulf of Suez

Fahmy et al. (2005) studied the distribution of Chl *a* in the Gulf of Suez and found that the average concentration in the main body of the Gulf (from 11 stations in an annual cycle) was only 0.19 μg L^{-1}, somewhat of the same order as

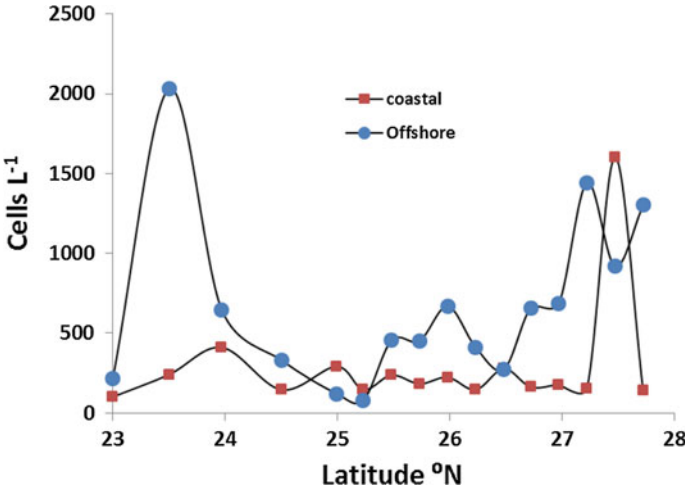

Fig. 27.16 Spatial distribution of the microphytoplankton abundance (diatoms and dinoflagellates) in the offshore (blue) and coastal (red) stations during the 2012 cruise

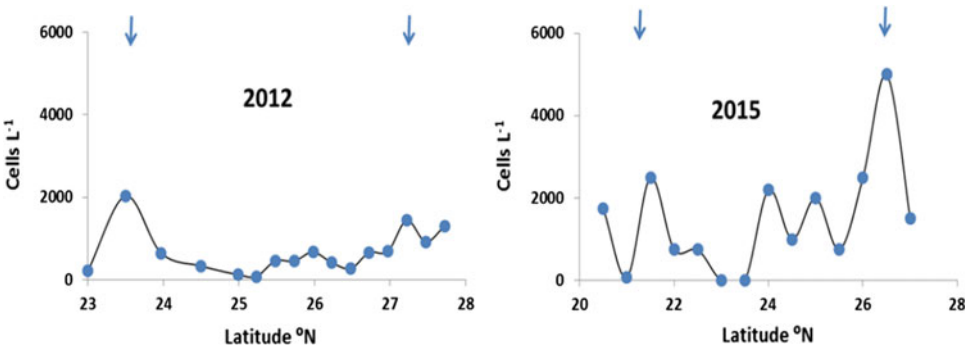

Fig. 27.17 Spatial distribution of the microphytoplankton (diatoms and dinoflagellates) of the Red Sea during the 2012 and 2015 cruises (see Fig. 27.1). Arrows indicate the locations of the zonal currents

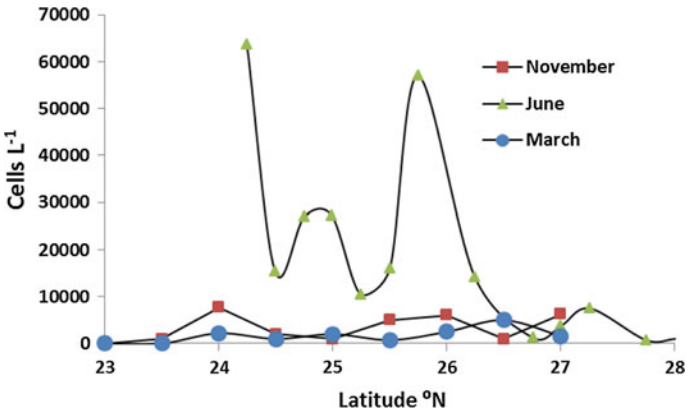

Fig. 27.18 Spatial distribution of the microphytoplankton (diatoms and dinoflagellates) abundance during Autumn-Winter (November, red), Summer (June, green) and Spring (March, blue) in the 2012 to 2015 cruises in the Red Sea (see Fig. 27.1)

observed in the Gulf of Aqaba. Only at three stations in the extreme north of the Gulf of Suez, did the average increase to 1.87 μg L^{-1}, a condition attributable to human impacts.

Conclusions

Our current knowledge of phytoplankton and the productivity of the Red Sea can be summarized as follows. The levels of biomass and production are relatively low, yet with a discernable north-south gradient. The distributions of phytoplankton biomass and productivity are also influenced by anticyclonic eddies which entrain nutrient-rich GAIW across the Red Sea basin. The injection of nutrients into the euphotic zone in the eddy boundary currents favours the proliferation of producers across a range of size classes rather than a single class. Biomass and production in these areas are twice as high as elsewhere in the Red Sea, suggesting the notion that the Red Sea is oligotrophic needs to be revised. As with any nutrient-poor tropical sea, the

primary production in the Red Sea is supported up to 80% by nano- and picoplankton. Although the contributions of microplankton (diatoms and dinoflagellates) appear to be less significant, the phytoplankton diversity is quite high, with nearly four hundred species identified so far.

The purpose of this review, besides summarizing the state of the knowledge, is also to reflect on prospective areas of research. With respect to primary production, the conclusions on eddy-influenced patterns of higher phytoplankton abundance and production are derived only from data collected in the eastern half of the Red Sea. Thus, to study whether such a pattern can be traced in the western half as well would be worthwhile. Secondly, the importance of coral reefs (and the associated macroalgal communities) that border almost the entire coastline of the Red Sea in enhancing the overall productivity of the Red Sea needs to be quantified. Thirdly, the importance of benthic primary production has not been studied. With clear waters permitting maximum penetration of sunlight, benthic primary production can be a significant contributor to the overall productivity. Finally, the importance of *Trichodesmium* spp., after which the Red sea has been named, in the overall productivity of the Red Sea (Naqvi et al. 1986), or of dust-borne nutrients (Wafar et al. 2016b), still remain conjectural.

In terms of composition and identification of the various algal groups, several more genera and species may still remain to be identified. For example, the inventory of 181 species made by Halim (1969) and in existence since the turn of 19th century increased dramatically to 389 species within the next 40 years, mainly through the compilation by Ismael (2015), and by a further 74 species from an analysis of the samples collected during the KFUPM cruises. It would be possible to enlarge the current inventory with more efforts in sample collection and identification. Besides, what we know of phytoplankton species is limited at present mainly to species composition of microplankton cells (>20 μm) and information on nano- and picoplankton as well as benthic primary producers (e.g., benthic diatoms in the sediments) is almost non-existent.

Qurban et al. (2014) concluded that the high levels of production in the <20 μm fraction of plankton and the perceived potential for the flux of N through heterotrophy suggests a greater role for the microbial loop in trophic dynamics of the Red Sea. However, in a later study Qurban et al. (2017) could not find a clear a pattern of association between variations in the proportion of nutrients taken up by smaller cells (<20 μm) and the flux of nutrients into the euphotic zone. Taken together, these would suggest that the energy flux through the microbial loop within the euphotic zone would still remain an important pathway in the trophic dynamics of the Red Sea at any time. Further quantification of this at wider spatial and temporal scales could better define the trophic status at primary levels and enable a prediction of their possible responses to nutrient enrichment.

Beyond what was discussed above, the most alluring avenue of research would be in the context of global change. As mentioned above, the Red Sea is one of the warmest and saltiest of all the world's seas, and these environmental conditions are forerunners of what they would be in other regions when the effects of global warming start to be manifested. The Red Sea thus can be considered a natural laboratory where the variation of physiological responses of phytoplankton as a function of temperature and other environmental conditions (e.g., salinity, pH, UV radiation etc.) using natural plankton assemblages may enable us to understand and forecast how plankton systems in other seas might respond to climate changes.

Acknowledgements We thank the Center for Environment and Water, Research Institute, King Fahd University of Petroleum and Minerals, Dhahran, Saudi Arabia, for encouragement and support.

References

Acker J, Leptoukh G, Shen S, Zhu T, Kempler S (2008) Remotely-sensed chlorophyll *a* observations of the northern Red Sea indicate seasonal variability and influence of coastal reefs. J Mar Syst 69:191–204

Al-Harbi SM, Khomayis HS (2010) Eutrophication and chlorophyll-a in a severely polluted coastal water of Jeddah, Red Sea. JKAU Mar Sci 21:15–29

Baars MA, Schalk PH, Veldhuis MJW (1998) Seasonal fluctuations in plankton biomass and productivity in the ecosystems of the Somali current, Gulf of Aden, and southern Red Sea. In: Sherman K, Okemwa E, Ntiba M (eds) Large marine ecosystems of the Indian Ocean: assessment, sustainability, and management. Blackwell Science, Oxford, pp 143–174

Badran MI (2001) Dissolved oxygen, chlorophyll a and nutrients: Seasonal cycles in waters of the Gulf Aqaba, Red Sea. Aquat Ecosyst Health Manage 4:139–150

Badran MI, Foster P (1998) Environmental quality of the Jordanian coastal waters of the Gulf of Aqaba, Red Sea. Aquat Ecosyst Health Manage 1:75–89

Badran M, Rasheed M, Manasrah R, Al-Najjar T (2005) Nutrient flux fuels the summer primary productivity in the oligotrophic water of the Gulf of Aqaba (Red Sea). Oceanologia 47:47–60

Churchill JH, Bower A, McCorkle DC, Abualnaja Y (2014) The transport of nutrient-rich Indian Ocean water through the Red Sea and into coastal reef systems. J Mar Res 72:165–181

Dham VV, Wafar M, Heredia AM (2005) Nitrogen uptake by size-fractionated phytoplankton in mangrove waters. Aquat Microb Ecol 41:281–291

Dorgham MM, El-Sherbiny MM, Hanifi MH (2012) Environmental properties of the southern Gulf of Aqaba, Red Sea. Egypt. Medit Mar Sci 13:179–186

Edwards FJ (1987) Climate and oceanography. In: Edwards AJ, Head SM (eds) Key environments: Red Sea. Pergamon Press, Oxford, pp 45–70

Elawad AES (2012) Study of inter-annual variability of chlorophyll in the Red Sea. Thesis, University of Bergen, M.Sc, p 49

Fahmy MA (2003) Water quality in the Red Sea coastal waters (Egypt): analysis of spatial and temporal variability. Chem Ecol 19:67–77
Fahmy MA, Sheriadah MA, Soeud AA, Rahman SMA, Shindy M (2005) Hydrography and chemical characteristics of the coastal water along the Gulf of Suez. Egypt J Aquat Res 31:1–14
Halim Y (1969) Plankton of the Red Sea. Oceanogr Mar Biol Ann Rev 7:231–275
Ismael AA (2015) Phytoplankton of the Red Sea. In: Rasul NMA, Stewart ICF (eds) The Red Sea: the formation, morphology, oceanography and environment of a young ocean basin. Springer Earth System Sciences, Berlin Heidelberg, pp 567–583
Khmeleva NN (1970) On the primary production in the Red Sea and the Gulf of Aden. Biol Morja Kiew 21:107–133
Khomayis HS (2002) The annual cycle of the annual cycle of nutrient salts and chlorophyll-a in the coastal waters of Jeddah, Red Sea. J King Abdulaziz Univ Mar Sci 13:131–145
Labiosa RG, Arrigo KR, Genin A, Monismith SG, van Dijken G (2003) The interplay between upwelling and deep convective mixing in determining the seasonal phytoplankton dynamics in the Gulf of Aqaba: Evidence from SeaWiFS and MODIS. Limnol Oceanogr 48:2355–2368
Lenz J, Schneider G, El Hag AGD, Gradinger R, Fritsche P, Moigis A, Pillen T, Rolke M, Weisse T (1988) Planktonological data from the central Red Sea and the Gulf of Aden—RV 'Meteor', cruise No. 5/2, January-March 1987. Ber Inst Meereskde Kiel 180
Levanon-Spanier I, Padan E, Reisis Z (1979) Primary production in a desert-enclosed sea—the Gulf of Elat (Aqaba), Red Sea. Deep-Sea Res 26:673–685
Longhurst A, Sathyendranath S, Platt T, Caverhill C (1995) An estimate of global primary production in the ocean from satellite radiometer data. J Plankton Res 17:1245–1271
Maillard C, Soliman GF (1986) Hydrography of the Red Sea and exchanges with the Indian Ocean in summer. Oceanol Acta 9:249–269
Malone TC (1980) Algal size. In: Morris I (ed) The physiological ecology of phytoplankton. Univ Calif Press, pp 433–464
Naqvi SWA, Hansen HP, Kureishy TW (1986) Nutrient uptake and regeneration rations in the Red Sea with reference to the nutrient budgets. Oceanol Acta 9:271–275
Petzold M (1986) Untersuchungen zur horizontalen und vertikalen Verteilung des Phytoplanktons in Roten Meer. Univ Hamburg, Diplomarbeit Institut fur Hydrobiologie und Fischereiwissenschaft
Quadfasel D, Baunder H (1993) Gyre-scale circulation cells in the Red Sea. Oceanol Acta 16:221–229
Qurban MA, Balala AC, Kumar S, Bhavya PS, Wafar M (2014) Primary production in the northern Red Sea. J Mar Syst 132:75–82
Qurban MA, Wafar M, Jyothibabu R, Manikandan KP (2017) Patterns of primary production in the Red Sea. J Mar Syst 169:87–98
Raitsos DE, Pradhan Y, Brewin RJW, Stenchikov G, Hoteit I (2013) Remote sensing the phytoplankton seasonal succession of the Red Sea. PLoS ONE 8(6):e64909. https://doi.org/10.1371/journal.pone.0064909
Rasheed M, Badran MI, Richter C, Huettel M (2002) Effect of reef framework and bottom sediment on nutrient enrichment in a coral reef of the Gulf of Aqaba. Mar Ecol Prog Ser 239:277–285
Shaikh EA, Roff JC, Dowidar NM (1986) Phytoplankton ecology and production in the Red Sea off Jiddah, Saudi Arabia. Mar Biol 92:405–416
Slawyk G, Collos Y, Auclair J-C (1977) The use of the 13C and 15 N isotopes for the simultaneous measurement of carbon and nitrogen turnover rates in marine phytoplankton. Limnol Oceanogr 22:925–932
Souvermezoglout E, Metzl N, Poisson A (1989) Red Sea budgets of salinity, nutrients and carbon calculated in the Strait of Bab-El-Mandab during the summer and winter seasons. J Mar Res 47:441–456
Stambler N (2005) Bio-optical properties of the northern Red Sea and the Gulf of Eilat (Aqaba) during winter 1999. J Sea Res 54:186–203
Wafar M (2016) A note on the flow of Gulf of Aden Intermediate Water in the Red Sea. J Mar Sys 163:125
Wafar M, Ashraf M, Manikandan KP, Qurban MA, Kattan Y (2016a) Propagation of Gulf of Aden Intermediate Water (GAIW) in the Red Sea during autumn and its importance to biological production. J Mar Sys 154:243–251
Wafar M, Qurban MA, Ashraf M, Manikandan KP, Flandez AV, Balala AC (2016b) Patterns of distribution of inorganic nutrients in Red Sea and their implications to primary production. J Mar Sys 156:86–98
Weikert H (1987) Plankton and the pelagic environment. In: Edwards A, Head SM (eds) Red Sea. Pergamon Press, Oxford, Key Environment Series, pp 90–111
Yentsch CS (1965) Distribution of chlorophyll and phaeophytin in the open ocean. Deep-Sea Res 12:653–666
Yentsch CS, Wood L (1961) Measurements of primary productivity in the Red Sea, Gulf of Aden and Indian Ocean. Woods Hole Oceanographic Institution, Ref. 61–6, Appendix 8:6
Zhan P, Subramanian AC, Yao F, Hoteit I (2014) Eddies in the Red Sea: a statistical and dynamical study. J Geophys Res Oceans 119. https://doi.org/10.1002/2013jc009563